The Astronomical Review, 2012, Vol. 7, No. 1, 4-24

An Interferometrically Derived Sample of Miras with Phase using Spitzer: Paper I – A First Look

M. J. Creech-Eakman[1], T. Güth[1], D. G. Luttermoser[2], C. A. Jurgenson[3], A. K. Speck[4]

1 – New Mexico Tech, Department of Physics, 801 Leroy Place, Socorro, NM, 87801

2 – East Tennessee State University, Department of Physics and Astronomy, Box 70652, Johnson City, TN, 37614

3 – New Mexico Tech, Magdalena Ridge Observatory, 801 Leroy Place, Socorro, NM, 87801

4 – Univ. of Missouri, Department of Physics and Astronomy, Columbia, MO, 65211

Abstract: We show preliminary 10-37 micron high-resolution spectra taken with the Spitzer Space Telescope in 2008-9 of Mira variables distributed across the M, S and C chemical subclasses. Our complete sample of 25 galactic Miras was observed from two to several times during this Spitzer campaign and all have simultaneously measured near-infrared interferometric diameters acquired using the Palomar Testbed Interferometer. Because our sources are very bright for Spitzer IRS (typically 5-100 Janskys), we have excellent signal to noise and for many sources see marked changes in overall flux levels as a function of phase. Further, we are able to identify many strong emission lines and emission features due to silicate and carbon dusts and molecular constituents. We introduce the sample and the design of our experiment, discuss the data reduction required for such bright sources using Spitzer, show several examples of spectra with phase and discuss some preliminary findings.

1. Introduction:

Asymptotic Giant Branch (AGB) stars are low to intermediate-mass stars in the final stages of their evolution. They are characterized by H and He nuclear burning shells atop an electron degenerate core of C and O ash. Instabilities in the shell burning layers cause acoustically driven pulsations which loft the atmosphere away from the stellar surface. Convection mixes the burning constituents, and occasionally results in a process called “dredge up” which mixes the stellar ash throughout the AGB atmosphere. The pulsational instabilities can be regular or irregular; in the case of regular instabilities, astronomers observe a regular pulsation period typically of 200-500 days, characteristic of a Mira variable. If the acoustic pulsations are only somewhat regular or show no regularity, they are referred to as Semi-Regular Variables or

Irregular Variables. These acoustic pulsations are readily recognized at optical wavelengths, where a Mira variable may vary up to 8 magnitudes during its pulsational period. Lofting of the atmosphere results in mass-loss from the star, reaching as high as 10^{-5} M_o yr^{-1}. Depending upon the initial mass of the progenitor and other details of the evolution, the AGB star may survive the mass-loss and thermal-pulse evolution long enough to evolve from a star that produces atmospheric constituents with a C/O ratios less than 1, through a phase where C/O ~1, and eventually where C/O ratios are greater than 1. This sequence is mainly attributable to how much C or O is left over after most of the gaseous constituents have been trapped as CO. These stars are referred to as O-rich or M-type, S-type, and C-rich (R, N or C spectral types) or Carbon stars, and all may exhibit regular or irregular pulsation. The molecular constituents formed in their atmospheres are lofted out of the star's gravitational well, cooling and forming various solid-state constituents typically referred to as dusts. These dusts make up the majority of the material returned by stars to the interstellar medium and create characteristic signatures in the infrared spectra of AGB stars. AGB stars represent an important stage of stellar evolution, one which is complex to observe and even more so to model. For excellent review articles on AGB evolution, nucleosynthesis and carbon stars, see Herwig (2005), Busso et al. (1999), Wallerstein & Knapp (1998), Habing (1996) and Iben & Renzini (1983).

Below we discuss the design and intent of our experiment, the sample itself, and the data acquisition and reduction processes. In section 5, we show data for four Miras and discuss the details of the observations and preliminary insights based on the dataset, including trends in emission lines and broader spectral features in Section 6. In the final section of the paper we talk about the plans for continuing our modeling and analysis of this dataset.

2. The Experiment:

The Spitzer Space Telescope (Werner et al 2004) Infrared Spectrograph (IRS) (Houck et al 2004) spectral data acquired here are part of a larger experiment to attempt to completely characterize the circumstellar atmosphere and dust environment of a group of Mira variables. The reasoning behind the experiment is that, because Mira atmospheres and dust production are complex, simultaneous ground and space-based data needed to be acquired to constrain the state of the stellar photosphere, atmosphere and dust producing region. Our approach relied on having ground-based optical interferometry in the K-band (centered at 2.2 microns) at the Palomar Testbed Interferometer (PTI) (Colavita et al. 1999) to constrain the photospheric size. The world-wide amateur community of variable star observers, represented in databases maintained by the AAVSO and AFOEV, are able to track the optical magnitude changes for most Miras observable by PTI throughout a majority of their cycles. Besides the basic pulsational characterization, these data can also be indicative of "dust events" (Kotnik-Karuza et al. 2006).

Spitzer spectral data are best used to examine the cooler portions of the stellar atmosphere and the circumstellar environment, in particular the dust condensation products being formed from the gas. It has long been noted that the ultraviolet, visible, and near-infrared spectra of Mira variables change over a pulsation cycle (e.g., Merrill 1940, Luttermoser & Bowen 1990; Luttermoser 1996; Castelaz & Luttermoser 1997; Castelaz et al. 2000). In the longer infrared spectral regime offered by Spitzer, it is important that various Miras of different spectral types (i.e., M, S, and C) be sampled at different phases through their pulsation cycles to see if such variation exists at these wavelengths too. A "typical" Mira has a pulsational period of approximately one year, and so the optimal sampling with Spitzer and PTI was determined to be approximately 1 month, such that the environment could be sampled at intervals of approximately 0.1 pulsational phase.

Distance information, which can be estimated in a number of ways including via Period-Luminosity relationships (c.f. Whitelock et al. 2008; Kanbur et al. 1997; Alvarez et al. 1997), parallax measurements (Knapp et al. 2003) or by using stellar masers (c.f. Vlemmings & van Lengevelde 2007; Kurayama et al. 2005), can be used, along with the PTI-derived photospheric angular size, using the relation:

$$T_{eff} = 2341*(F_{bol}/\Theta^2)^{1/4}$$

to determine an effective temperature and physical size of the atmosphere at the average location of the flux zone emitting at 2.2 microns in the star (where F_{bol} is in erg cm^{-2} sec^{-1} and Θ is in milliarcseconds). With both a physical diameter and temperature, a much more accurate determination of the underlying photospheric temperature than can be determined than would be possible using canonical spectral-type-derived temperatures. Modeling the atmosphere of Mira variables is difficult as described by Luttermoser (2009), however over the past few decades, significant progress has been made (e.g., Bowen 1988; Fleischer et al. 1992; Höfner et al. 1995; Höfner et al. 2003; Nowotny et al. 2010). The data collected here will be fundamental in understanding the atmospheric structure of these stars. As described below (Section 7), this dataset will be used to help constrain future atmospheric modeling of these stars. All components can then be traced with time and phase of the variable star to allow insights into the interplay between pulsational cycle, photospheric size, and production of dust in the Mira. Clearly this process must be iterative, requiring a great deal of collaborative work between various teams who are expert in the techniques and codes being used. We are just now in the early stages of this investigation (Creech-Eakman et al. 2009).

3. The Sample:

A long-term project was launched in 1999 using the Palomar Testbed Interferometer (PTI) to study the pulsational behavior of a group of over 100 Mira and semi-regular variable stars

across chemical subtypes and large range of periods (Creech-Eakman & Thompson, 2009). In order to be feasibly characterized with respect to phase, the majority of the stars varied between 2nd and 4.5th magnitude at K-band, with angular sizes between 2.0 and 5.0 milliarcseconds. For those stars with distance estimates, the majority of the sample is distributed between 1 and 3 kpc away. The entire PTI study continued through 2005, with a sub-sample continued thereafter to support this work with Spitzer. From the PTI subsample, approximately 40 stars with excellent phase coverage were selected for study with Spitzer IRS, however observational constraints with the spacecraft (especially the need for dedicated backgrounds) limited us to this slightly smaller sample. Because approximately 70% of the PTI sample was O-rich stars, this sample is also distributed in the same way. When choosing stars to observe with Spitzer, we attempted to maximize PTI coverage, Spitzer observing windows, and the ability to simultaneously observe from the ground and space (i.e. solar location).

4. Data Acquisition and Reduction:

The data were acquired during Spitzer GO program 50717, and the acquisition and reduction processes are described below for the data discussed herein.

4.1 Data Acquisition:

Stars were selected from the PTI interferometric sample such that: a) IRAS LRS data existed, and if possible, the stars were categorized as to dust spectral-subtype by Little-Marenin & Little (1990) or Sloan & Price (1998); b) the stars were in optimal observing windows for Spitzer such that they could be observed a few to several times during Spitzer cycle 5; and c) the stars were bright enough to have excellent SNR, but not so bright that they were likely to saturate Spitzer IRS (ideally in the 5-50 Jansky range), though predicting this was somewhat problematic since the stars are variable. We were aware that this last point would necessitate the use of defringing algorithms to reduce the data. As such, dedicated backgrounds were taken for all stars as recommended by the Spitzer IRS team. In cases where the stars might be faint enough, low-resolution data were also acquired, especially at the shortest wavelength end of IRS so that the 5-10 micron range could be well-characterized for the stars.

All stars shown here have short and long high-resolution IRS spectra (SH and LH), while some also have short or long low-resolution data (SL or LL), as noted in Table 1. To date we have reduced nearly all high-resolution data, with the exception that some data show unusual features due to saturation and/or large mismatches (which we are dubbing “the offset issue”) between the short and long wavelength high-resolution modules.

4.2 Data Reduction:

The first step of the data reduction procedure was to subtract the dedicated background spectral image from the stellar spectral image, which produced a sky subtracted stellar spectral image. This was performed in IDL and using it we removed the background from the Image files (*_bcd.fits), as well as from the Mask files (*_bmask.fits) and the Uncertainty files (*_unc.fits).

Next we used the Spitzer IDL package IRSCLEAN to remove any rogue/bad pixels in these subtracted images. We not only removed the bad pixels automatically flagged by the program, but also those flagged additional by hand in all spectra, providing a much cleaner spectrum for each ABG star. To extract the stellar spectra from the stellar spectral image, we used the "Spitzer IRS Custom Extractor" (SPICE) tool. The standard procedure, which assumed a regular extraction of a point source, was implemented for all our sky subtracted and cleaned images. By using the bad pixel masks as well as other calibration data that come with our observations and is specific to the orbits and GO cycles, the SPICE package can extract and flux calibrate the IRS spectra. It should be noted that version of the calibration files used by SPICE need to be consistent with the version of the pipeline used to process the data.

Since all our AGB stars were bright, fringes produced internally within the spacecraft might have been introduced in our spectra during the observations. Hence, we next used the Spitzer IRSFRINGE tool to "defringe" each spectrum at this step. By default, IRSFRINGE removes both the primary and secondary fringe components automatically using a Fourier transform technique.

Next, the individual spectral orders needed to be reassembled into one complete high-resolution spectrum. This was accomplished via our own IDL code to remove these order overlaps at certain wavelengths. No relevant data were deleted during this part of the process. For reference, band edges of the different orders across the IRS spectra occur in the SH mode at: 10.3852, 10.9597, 11.5927, 12.3096, 13.1111, 14.0293, 15.0813, 16.3248 and 17.7526 microns, and in the LH mode at: 19.7783, 20.8444, 22.0597, 23.4433, 24.9553, 26.7202, 28.7773, 31.0703 and 33.7704 microns, as described in the IRS Data Reduction Cookbook. The last step of the data reduction procedure was to combine the individual nods of each module to create the final spectrum of each AGB star. First, the IRAF (Image Reduc tion and Analysis Facility maintained at NOAO) program rspectect (IRAF package onedspec) was used to create fits files. These files were then combined using the IRAF program imcombine. To create postscript files for the final spectra seen here, we extracted the flux values using the IRAF program wtextimage and then plotted those values versus their corresponding wavelengths. We present four panels of spectra below (Figures 1-4) along with information about phase and chemical subtypes in Table 1.

Here we offer a few comments about the outstanding data reduction issues. As recommended by the Spitzer Science Center and the Cookbook data reduction procedures, we have tried to use the Spitzer program dark_settle to correct, or at least reduce, offsets seen between SH and LH data. In no case did this achieve the desired, or even measurable, results. Therefore other processes will be implemented to attempt to correct the offsets. These data are labeled "offset issue" in Table 1. The saturated data cannot be recovered, and therefore we have chosen to plot only those data which are clearly not saturated. Saturation typically occurs at wavelengths short of 13 microns in the SH module. Finally, some of the SH data look anomalously "flat", almost as though a gain setting were different for these data. We are still trying to determine a diagnosis for these data, and so they are labeled "SH data issue" below. Stars with an '*' following the dust chemical subtype were typed by the authors. Phases and periods were derived from examining AAVSO and AFOEV data for the PTI portion of our program, and were derived independently from these data and assigned an epoch near 1999 when the PTI portion of the project started.

Table 1: Acquired Spitzer Data

Star Name	**Date**	**Phase/Period /Epoch**	**Chemical Subtype**	**Notes/Issues**
S Peg	2008-08-12	51995; 312.2d; 0.631	M – SE1	
S Peg	2009-01-05	0.098		
R Tri	2008-09-07	51370; 275.3d; 0.153	M – SE3	
R Tri	2008-10-02	0.222		
S Ser	2008-08-13	51338; 389.0d; 0.620	M – SE3	
S Ser	2008-09-02	0.671		
S Psc	2008-08-12	52158; 422.7d; 0.990	M – SE4	
S Psc	2008-09-03	0.042		
Y Del	2008-07-11	51199; 475.1d; 0.280	M – SE4	
Y Del	2008-11-11	0.539		
Y Del	2008-11-30	0.579		
RV Peg	2008-07-11	51794; 393.5d; 0.278	M – SE7	Offset issue

RV Peg	2008-08-08	0.349		Offset issue
RV Peg	2008-12-14	0.674		SH data issue
RV Peg	2009-01-05	0.730		SH data issue
U Cvn	2008-06-05	52175; 307.9d; 0.948	M – SE7	Offset issue
U Cvn	2008-07-02	0.036		Offset issue; SL & LL data
UX Cyg	2008-07-11	52350; 546.3d; 0.225	M – SE8	Saturation: started at 13.0 microns
UX Cyg	2008-08-08	0.276		Saturation: started at 13.0 microns
UX Cyg	2008-11-13	0.454		Saturation: started at 13.0 microns
UX Cyg	2008-12-01	0.487		Saturation: started at 13.0 microns
Z Cyg	2008-06-05	51492; 267.0d; 0.725	M – SE8	Offset issue
Z Cyg	2008-07-11	0.859		Offset issue
Z Cyg	2008-08-07	0.961		Offset issue
Z Cyg	2008-09-01	0.054		Offset issue
Z Cyg	2008-10-02	0.170		Offset issue
Z Cyg	2008-11-08	0.309		Offset issue
Z Cyg	2008-11-30	0.391		Offset issue
R Cet	2008-09-03	51421; 165.8d; 0.850	M – SE8	
R Cet	2008-10-01	0.019		
RU Lyr	2008-06-05	51782; 369.1d; 0.694	M – no feature	SH data issue; SL & LL data
RU Lyr	2008-07-11	0.792		SH data issue
RU Lyr	2008-08-07	0.865		SH data issue
RU Lyr	2008-09-01	0.932		SH data issue
RU Lyr	2008-10-02	0.016		SH data issue
RU Lyr	2008-11-16	0.138		SH data issue
RU Lyr	2008-11-30	0.176		SH data issue
S Lac	2008-08-07	51249; 240.6d; 0.279	M – no feature	
S Lac	2008-09-01	0.383		

S Lac	2008-12-15	0.819		
W Her	2008-06-05	51482; 273.7d; 0.473	M – no feature	
W Her	2008-07-11	0.604		
W Her	2008-08-13	0.725		
W Her	2008-09-01	0.794		
W Her	2008-10-05	0.919		
RT Cyg	2008-06-05	52009; 191.4d; 0.654	M – no LRS	SL & LL data
RT Cyg	2008-06-29	0.780		SL & LL data
RT Cyg	2008-08-07	0.983		SL data
RT Cyg	2008-09-01	0.114		SL data
RT Cyg	2008-10-02	0.276		SL data
RT Cyg	2008-11-06	0.459		SL data
RT Cyg	2008-11-30	0.584		SL data
RY Lyr	2008-06-05	52175; 330.4d; 0.406	M – no LRS	SH data issue; SL & LL data
RY Lyr	2008-07-11	0.515		Offset issue; SL data
RY Lyr	2008-09-07	0.690		Offset issue; SL data
RY Lyr	2008-10-16	0.808		SH data issue; SL data
RY Lyr	2008-11-09	0.881		SH data issue; SL data
SS Cas	2008-08-15	52400; 143.1d; 0.029	M – no LRS	SL data
SS Cas	2008-09-04	0.169		SL data
SS Cas	2008-10-06	0.386		SL data
LX Cyg	2008-08-07	52164; 582.7d; 0.326	S – no LRS	SL data
LX Cyg	2008-09-01	0.369		SL data
LX Cyg	2008-12-05	0.532		SL data
LX Cyg	2009-01-05	0.957		SL data
R Cyg	2008-07-11	51400; 381.3d; 0.544	S – SE2	
R Cyg	2008-08-06	0.612		

R Cyg	2008-09-07	0.696		
R Cyg	2008-10-16	0.782		
R Cyg	2008-11-18	0.884		Saturation: started at 12.2 microns
R Cyg	2008-12-01	0.919		Saturation: started at 13.0 microns
S Lyr	2008-06-05	51653; 439.3d; 0.758	S – SE2	
S Lyr	2008-06-30	0.815		Offset issue; SL & LL data
S Lyr	2008-10-05	0.022		
S Lyr	2008-11-06	0.086		
S Lyr	2008-12-02	0.168		
S Uma	2008-06-05	52072; 231.0d; 0.814	S – no LRS	SL & LL data
S Uma	2008-07-01	0.152		SL & LL data
S Uma	2008-12-15	0.874		SL data
X And	2008-08-12	51945; 217.9d; 0.596	S – no feature	
X And	2008-09-04	0.701		
RZ Peg	2008-07-04	2454651	C – Br1*	SL & LL data
RZ Peg	2008-08-06	2454684		
RZ Peg	2008-12-11	2454811		Possible saturation
U Lyr	2008-06-05	52531; 457.3d; 0.572	C – Br1	SL & LL data
U Lyr	2008-07-11	0.653		
U Lyr	2008-08-07	0.710		
U Lyr	2008-09-10	0.784		
U Lyr	2008-10-02	0.819		
U Lyr	2008-11-06	0.909		
V Crb	2008-07-01	51319; 371.6d;0.960	C – SiC	SL & LL data
V Crb	2008-08-13	0.073		
V Crb	2008-09-02	0.127		
ZZ Gem	2008-11-11	52956; 319.0d; 0.720	C – Br1/2*	SL data

ZZ Gem	2008-12-02	0.786		SL data

5. Preliminary Results:

Below we show and discuss a brief background and spectral panels for four Miras in our sample, two different M-types, one S-type, and one C-type Mira. In each case, details about the pulsational phase and data reduction are included in Table 1 above.

5.1 M-Type Mira Y Delphini

Y Del (M8e) was initially identified as a Mira-type variable by Campbell (1926). While it has been studied in several maser searches (c.f. Sivagnanam et al, 1988; Lewis et al. 1990; Lewis, 1997), no oxygen-rich masers have been identified in the circumstellar environment. It was observed with IRAS Low-Resolution Spectrometer (LRS) and typed as having an "SE4t" type silicate emission feature by Sloan & Price (1998), having a broad emission feature peaking at 10 microns and slowly decreasing past 13 microns, but with a 13 micron emission peak (the "t"), in continuum subtracted data. It was additionally observed using the CGS3 spectrometer on UKIRT (Speck et al. 2000) and typed to have a 10 micron silicate feature (silicate AGB-C in their Table 3) that tends to have narrower spectral features.

For Y Del, we have three spectra spanning about 4 months and 0.3 of its pulsational phase. All three spectra exhibit the classic 10 and 18 micron features attributed to amorphous silicates. Again we do not see much change in the overall shape of the spectrum despite a decrease in the overall brightness of the star. The strengths and ratios of the 17 and 33 micron features do vary markedly. There are also features longwards of ~20 microns that may be molecular bandheads. These features do not appear in U Lyr or S Lyr (see below), which may suggest an O-rich chemical origin.

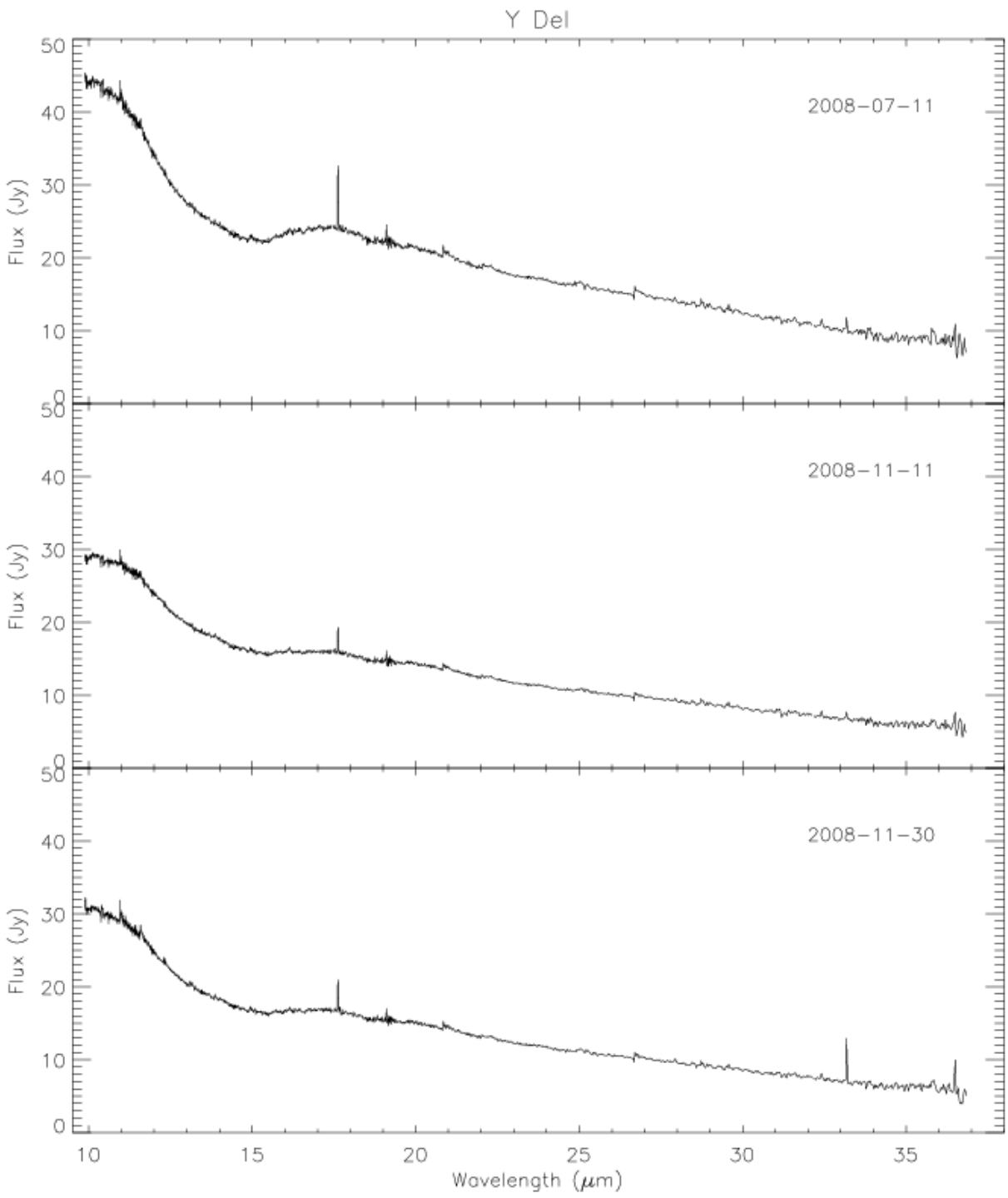

Figure 1: Three spectra of O-rich Mira Y Del from 0.280 to 0.579 pulsational phase.

5.2 M-Type Mira UX Cygni

UX Cyg (M4-6.5e) was first identified as a variable star having a peculiar spectrum by Pickering and Fleming (1905). It is known to have all three classes of oxygen-rich masers, SiO, H_2O and OH (c.f. Engels and Heske, 1989; Comoretto et al. 1990; Lewis 1997) and has been studied by many groups subsequently to understand the nature and motion of these masers. Its IRAS LRS spectrum was first typed by Little-Marenin & Little (1990) to be in the "Sil" feature class, having a broad classic silicate emission feature peaking at 9.8 microns. Sloan & Price (1998) reclassified it as an "SE8t", having a peaked emission near 10 microns with a fast drop off toward 12 microns, but with a 13 micron emission feature (again the "t"), in continuum subtracted spectra.

The Spitzer spectra of UX Cyg were so bright that the spectrum was saturated for wavelengths shortward of 13 microns. While we cannot see the expected 10 micron feature, there is clearly a feature around 18 microns which is not like the typical amorphous silicate feature. This solid state broad feature appears to be composed of two overlapping peaks – one at ~17.5 microns and one at 20 microns, both broad. This may suggest that there are two distinct silicates contained within the dust around UX Cyg. Alternatively, there are several metal (Mg and Fe) oxides which could give rise to features within this region (c.f. Speck et al. 2000). As with all the other spectra, the solid state features do not seem to vary much with time, whereas both the strengths and ratios of the emission lines at 17.6 microns and 33.2 microns change markedly from observation to observation.

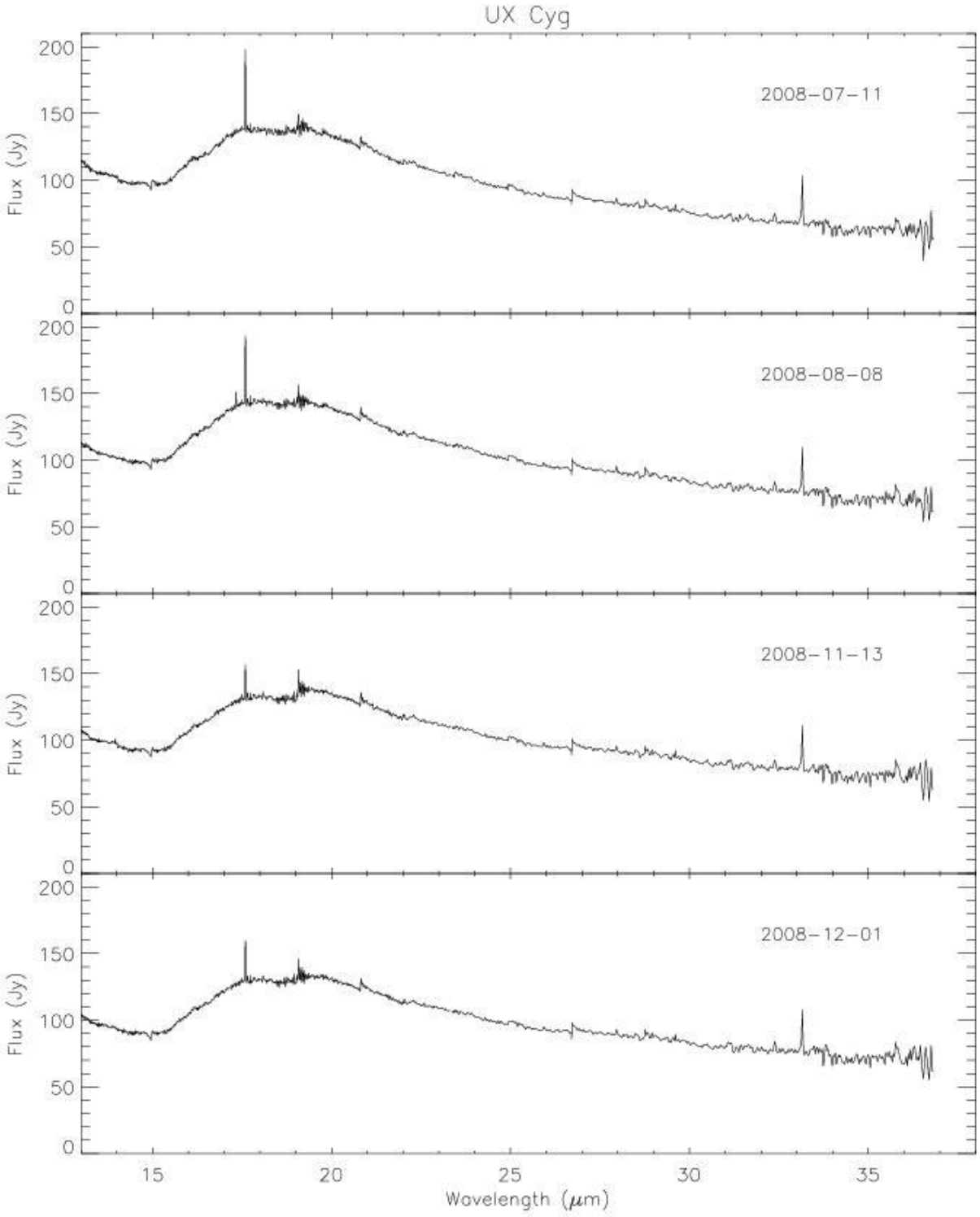

Figure 2: Spectra of O-rich Mira UX Cyg spanning 0.225 to 0.487 of the pulsational phase. Note that the spectra start at 13 microns as the detectors were saturated shortward of this wavelength.

5.3 S-Type Mira S Lyrae

S Lyr (CSe) was first identified as a variable star by Espin & Anderson (1894). It was typed as and SC star by Catchpole & Feast (1971) and catalogued as an S-star by Stephenson (1976). Little-Marenin & Little (1988) categorized it as an SC star based on its IRAS LRS spectrum. They show that the continuum-subtracted LRS spectrum is well-matched by a mid-infrared spectrum that blends both C and O-rich dust features (their Figure 3). It was also spectrally typed by Sloan & Price (1998) as an SE2, having a broad silicate emission feature peaking toward 10 microns. Because of the nature of S stars, there have been many attempts to spectrally type and verify S Lyrae's status as an S-type Mira (c.f. Noguchi et al. 1991; Jorissen et al. 1993). A recent study examines ISO SWS spectra of S Lyr and other S-type stars as compared to O-rich miras in the ISO archive and finds a very different presentation for the dust at this wavelength regime as compared to O-rich stars (Hony et al. 2009).

When first observed in June 2008, the spectrum of S Lyr displays a broad solid-state infrared feature around 11 microns, which is most likely due to SiC. This feature appears stronger in the subsequent observations as the star goes through its pulsational maximum (panel 3), as do the apparent emission lines 17.6 and 33.2 microns. There is also a hint of a broad feature around 17 microns and possible a weak 30 micron feature. Although S Lyr is classified as an S or CS-star, its spectrum indicates that the circumstellar dust is carbon-rich (c.f. U Lyr below). Furthermore, S Lyr shows a weak sharp emission feature at ~11 microns superposed on the broad SiC dust feature; the feature also appears in the spectra of U Lyr, but not in those of the (O-rich) M-stars above. The lack of changes in the spectra of S Lyr is consistent with recent observations of well-known carbon star, V Cyg. Although the overall brightness changes, the shape and strength of the solid state features are not strongly effected despite obvious changes in the ratios of the prominent emission lines.

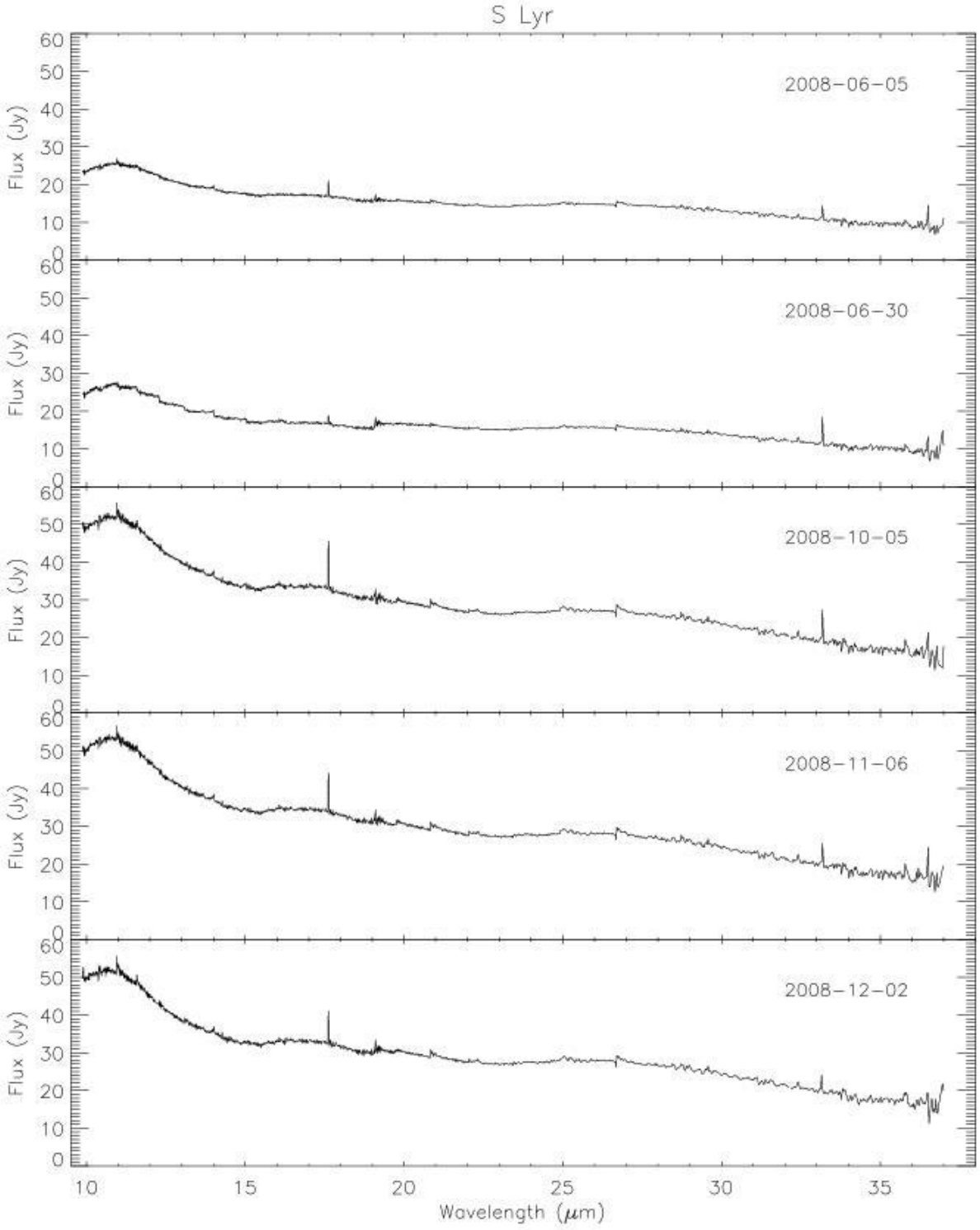

Figure 3: Five spectra of S Lyr covering from 0.758 through maximum to 0.168 pulsational phase. Note the change in the appearance of the spectrum as it goes through maximum in the third panel.

5.4 C-Type Mira U Lyrae

U Lyrae was first identified as a long-period variable star by Campbell (1926) and thereafter identified as C-rich (Merrill et al. (1933)). While it was observed by IRAS and has an LRS spectra (Olnon et al. 1986), no dust typing of U Lyr was undertaken in any of the literature. The authors have examined U Lyrae's LRS spectrum and believe it is most similar to a 'Br1' spectral type, described in Sloan et al. (1998).

The six spectra of U Lyr shown in Figure 4 were taken over the course of 5 months (about 1/3rd of a pulsational period) and yet show very little variation from observation to observation. There is a strong 11 micron solid state feature which is most likely due to silicon carbide (SiC). There is a hint of an absorption feature at 13.7 micron which is due to C_2H_2. While C_2H_2 is common in C-stars, this acetylene feature is remarkably strong considering that the dust shell is not optically thick. Similarly strong bands are seen for C stars in the LMC and SMC (Srinivasan et al 2010; Speck et al 2006) and in optically obscured galactic C stars. While the overall shape of the spectrum appears more or less unchanged, the strength and ratio of the emission lines at 17.6 and 33.2 microns do vary from observation to observation. In addition, U Lyr exhibits extra emission lines at ~11 microns and ~27 microns not seen in the O-rich (M-type) stars. The lack of change in the spectra over the course of a significant fraction of the star's pulsation cycle is consistent with recent observations of V Cyg, a well-known carbon star whose spectra have been studied for both temporal and spatial variations. For V Cyg, changes are lost in time and space suggesting that we see a very stable dust layer.

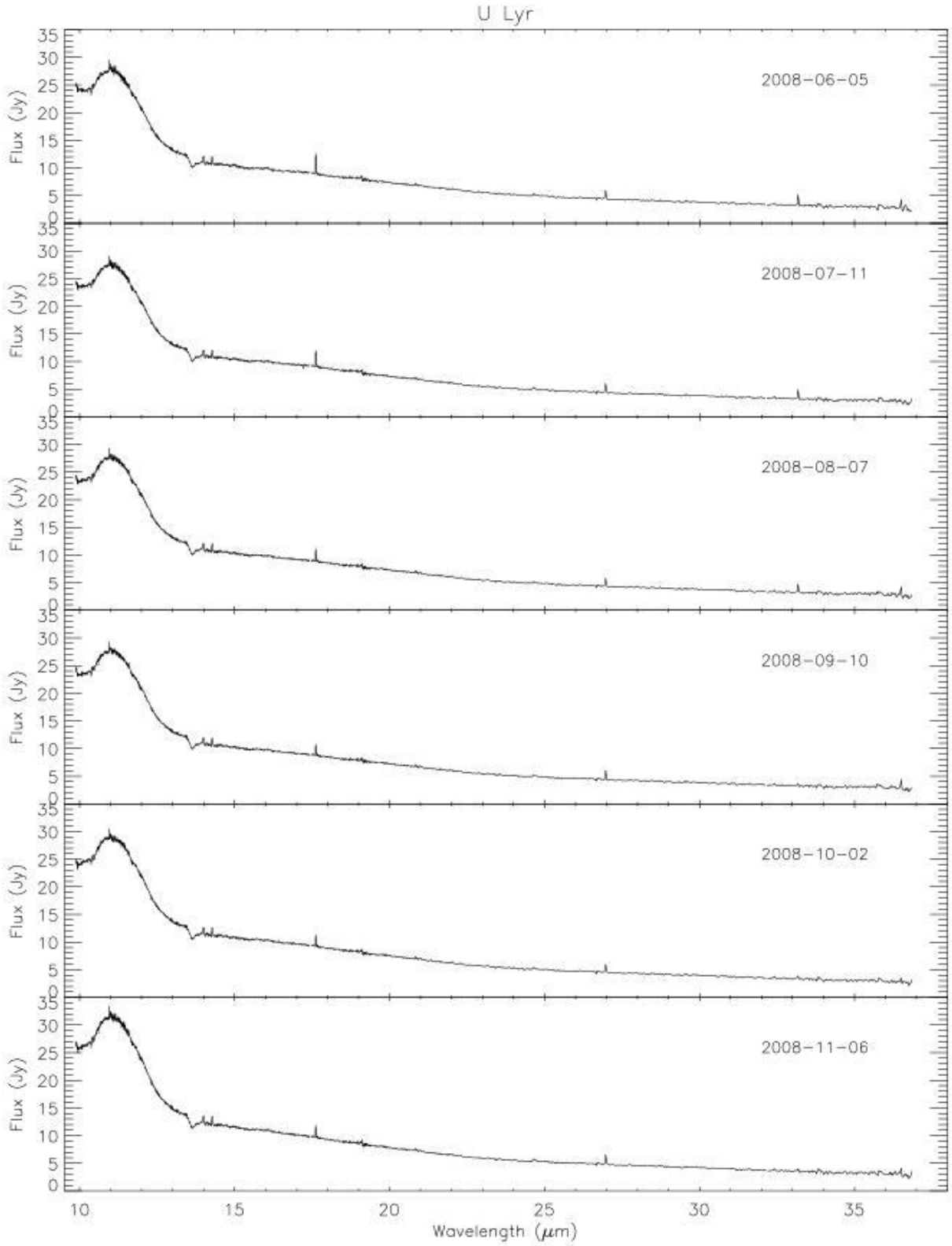

Figure 4: Six observations of U Lyr spanning 0.572 to 0.909 of the pulsational phase.

6. Initial Insights:

We have visually inspected and, using the IRAF splot package, investigated all the high-resolution spectra which we were able to reduce without significant uncertainties at the end of the processing. Several things are apparent in these spectra. In particular, certain strong emissions lines and broad features are seen in a large fraction of the spectra. These spectral features are more prevalent in certain chemical subtypes of the miras, and some of the features come and go, or in the case of a few spectral lines, go from absorption to emission, as the Mira pulsates. See Table 2 below for a brief cataloguing of features per star (inclusive of all phases of the data we have in hand). If the feature is in emission, we have labeled it with an "X", if in absorption with an "A", and if weakly in emission, with an "#". Stars with reduction issues that precluded such inspection are labeled "red. issues".

Table 2: Brief catalog of lines and features in the complete Spitzer dataset. Discussion of the symbols/notes can be found in the text.

Stars	**# spec**	**lines**												**broader features**					
M Stars		10.9	13.5	13.8	14.9	16.2	17.6	23.1	27	27.9	32.7	33.2	33.8	13.5 acet	19 unusual	10 broad	11 sharp	13 sharp	20 broad
S Peg	2	#		X	A	X	X					X			X			X	X
R Tri	2		#	X	A	X	X			X		X				X		X	X
S Ser	2	#		X	A	X	X			X		X			X			X	X
S Psc	2	#	X	X			X			X		X						X	X
Y Del	3	#					X					X			X				#
RV Peg	red. issues																		
U Cvn	2		X	X		X	X			X			X		X	X			X
R Cet	2		X	X		X	X			X		X	X		X	X			X
UX Cyg	4				A	X	X	#	X		X	X			X				X
Z Cyg	red. issues																		
RU Lyr	red. issues																		
S Lac	3	#	X	X	A	X	X			X		X	X		X	#		#	X
W Her	5	#	#	X		X	X				A	X	#		X	#		X	X
RT Cyg	7	#		X		X	X	A#		X	X	X	X		#				#
RY Lyr	red. issues																		
SS Cas	red. Issues																		
S Stars																			
LX Cyg	4	#					X					X		A	X	#	X		
R Cyg	6	#	#	#			X					X			#	#		#	#
S Lyr	5	#	#	#			X					X			#		#		#
S Uma	3	#					X					X			#			#	
X And	2	#					X					X			#			#	X
C Stars																			
RZ Peg	3	#					X					X					X		
U Lyr	6	X	X	X			X		X			X	#	A	X		X		
V Crb	3	X	A	X			X					X			X		X		
ZZ Gem	2	#					X					X		A	X		X		#

6.1 Spectral Lines:

Strong Emission Features: Since these are cool large stars, one should expect emission features to result from H I, He I, neutral metals, singly-ionized metals, and molecules. Since the radiation field from the star and its deeper shocks should be relatively cool (i.e., a brightness temperature less, and possibly much less, than 8000 K), the emission lines seen should result from either collisional or fluorescent processes similar to the emission lines seen at shorter wavelengths in these stars and not from recombination processes. Should a line result from a collisional process (e.g., Mg II h & k and Fe II (UV1, UV62, UV63) at ultraviolet wavelengths, H Balmer lines at visible wavelengths), one might favor lines arising out of levels of lower energy over lines collisionally excited out of higher energy levels. Since we are at wavelengths greater than 10 microns, this might suggest transitions that semi-forbidden and forbidden transitions to be more favorable in forming emission lines in these stars as compared to allowed transitions since collisional processes would favor such transitions. Meanwhile, there are many examples of emission lines fluoresced from strong collisionally excited lines (see Luttermoser and Bowen 1992; Luttermoser 2000). Fluoresced lines are pumped by photons from an emission line at a different wavelength from the fluoresced line (e.g., in the case of the Fe I (42) lines at 4202 Å and 4308 Å, Fe I (UV3) at 2795.006 Å absorb emission-line photons from the Mg II k line at 2795.523 Å, electrons then cascade back down a different transition giving rise to the Fe I (42) features which share the same upper level as this Fe I (UV3) transition). Further work will need to be performed to ascertain whether any of the emission lines seen result from fluorescent processes.

In addition to these items, lines associated with elements of higher abundance will be preferred over lines from lower abundance elements. Two sources were used to compile this line identification list: the ISO-SWS IR Spectral Line List (van der Hucht & Koornneef 1994) and the University of Kentucky Atomic Lines web interface (van Hoof 1999). The comments in the following tabulated data reflect the characteristics mentioned above listed in the following order: most likely, possible, and unlikely. Vacuum wavelengths are reported below.

Emission feature at 10.960 microns: This feature is fairly strong in the C stars, weak in the S stars, and weak or not present in the M stars. Its emission in the C and M stars stays relatively constant in time but shows variation in the S stars. This feature is likely due to either [Cr II] at 10.9579 microns (b 4P – b 4P, E_l = 29.951.88 cm^{-1} or Cr II] at 10.9654 microns (e 2G – z 4Ho, E_l = 62688.95 cm^{-1}. Unfortunately, there are many spin-forbidden Cr II] transitions in this spectral region, so it is unclear as to why some would show up as emission lines and others do not. He I transitions are considered unlikely for all the emission lines seen at these wavelengths since there are a large number of neutral helium transitions in this spectral regime, yet only a few

emission lines are seen, as well as the fact that these helium transitions all arise from very high energy levels. As a result of these facts, none of the lower abundance noble gas elements (e.g., Ne I and Ar I) were considered as likely candidates for these emission features.

Emission feature at 13.879 microns: This feature is very pronounced and relatively broad in the C stars and its flux stays relatively constant. It is present in S stars, but shows variation in time. It is very weak or not present in the M stars, though when present does show some variation in time. Due to these facts, this feature may be a blend of two neutral carbon lines at 13.8717 (1P – 1Do, E_l = 86912.86 cm^{-1}) and 13.872 microns (3/2[3/2] – 3Do, E_l = 87837.74 cm^{-1}) or due to [Cr II] at 13.8610 microns (a 4D – a 4G, E_l = 19,797.88 cm^{-1}).

Emission feature at 17.617 microns: This feature is the strongest emission line in all of the spectra. It shows substantial variation in time in the M and S stars, but stays relatively constant in flux in the C stars. The most likely candidate for this feature is [Ti II] at 17.6345 microns (a 4P - b 4P, E_l = 9363.62 cm^{-1}).

Emission feature at 32.691 microns: This feature is relatively weak in the C stars as compared to the M and S stars. Unfortunately, none of these transitions are more likely to represent the emission seen as compared to the others. The forbidden transition of [Fe II] at 32.7343 microns (a 2F – a2F, E_l = 27,314.92 cm^{-1}) is a likely candidate for this line.

Emission feature at 33.185 microns: This feature is seen in all of the spectral types and is relatively broad. Two neutral calcium lines are located at 33.185 and 33.187 microns. Should this feature be due to these two lines, perhaps some fluorescent process is causing these transitions to appear in emission. Two other possible identifications include [Fe II] at 33.0958 microns (b 4F – b 4F, E_l = 22,637.21 cm^{-1}) and the [V I] transition at 33.173 microns (b 4P – b 4P, E_l = 15,270.58 cm^{-1}).

While there are several other emission features in these spectra, including those tabulated in Table 2, we are still investigating the species that they could be and what makes sense in the context of the entire dataset. We are not entirely convinced that these lines are not influenced by artifacts of the data reduction process (for instance, beyond 35 microns where the spectra are known to be noisier).

Strong Absorption Features: In the wavelength regime of these spectra, it is likely that any strong absorption features seen will be due molecules involving relatively abundant species for a given spectral type. The strong feature near 13.7 microns in the carbon star U Lyr is due primarily to the Q, v5 band at 13.70978 microns of the C_2H_2 molecule, with perhaps some contamination of the n5 band of CHCH at 13.716 microns.

6.3 Broader Spectral Features:

Several broad and a few sharp features are seen in the spectra which are likely due to various solid state constituents in the circumstellar environments. The ones most readily identified are those known to be associated with the particular chemical subtypes. Readers should refer to Little-Marenin & Little (1988 & 1990), Sloan & Price (1998), Sloan et al. (1998), Speck (1998) and many other relevant papers for detailed discussions on solid state/dust features identified in AGB stars.

We start with the dusts attributed to silicates, typically with broad features seen from 9-12 and 18-20 microns, attributed to the stretch and bend of the Si-O bond (referred to in the Table 2 as "10 broad" and "20 broad"). While the 20 micron feature is seen in nearly all the M-star spectra, it's only barely visible in a few of the S and C stars. The 10 micron feature is a little more problematic to see without subtracting a continuum, but there does appear to be some feature at 10 microns in nearly all the spectra collected, likely not strictly attributable to silicates. Further investigation of 10 micron features will necessitate use of the SL data, where available, and continuum subtracted spectral modeling based on PTI derived temperatures.

Next we examine the 13 micron "sharp" feature. Spectral features in this location have been the subject of much discussion in AGB stars over the years, and have been attributed to Al_2O_3 (Vardya et al. 1986) and SiO_2 (Speck 1998) among M-type stars, and recently to SiS (Sloan et al. 2011) in S type stars. In this sample, the early silicate types ("SE1-4" class from Sloan & Price (1998)) tend to have a more obvious feature here, while the later "SE" types among the M Miras show no tendency for it. There is a hint of a feature in some of the S stars, but in none of the C stars in this sample. This may suggest that the feature has an oxygen related origin.

Carbon dusts have many features, one of the most important of which is due to SiC, a "sharp" feature at 11 microns. This feature is seen in all the C-type Miras, and tentatively in a few of the S-type Miras, one of which we show here (S Lyr – Figure 3). It is frequently, but not always, accompanied by an absorption feature mainly attributable to C_2H_2 at 13.5 microns in absorption.

Finally, we note an unusual feature in most of the spectra near 19 microns. We are not clear on the origin of this feature and it is possible that it may be an artifact of the data reduction process as it is near to the place where the SH and LH spectra are joined. This feature and many other features in these spectra will be investigated in the course of the next steps of this study, as described below.

7 The Next Steps:

The spectral and interferometric data reported here will be used to help constrain atmospheric models of these stars using a two-fold approach. First, detailed identifications will be made of the many of the emission lines, absorption lines and broad spectral features seen in these spectra. The strength of these features will then be empirically determined by fitting an appropriate blackbody to the continuum.

While this work is progressing, numerical modeling will be performed by using a combination of radiative transfer codes. As a starting point, radiative and convective equilibrium models will be determined for each star based upon its effective temperature, luminosity, radius, and mass through the use of the local thermodynamic equilibrium (LTE) code ATLAS (Kurucz 1970 & 1979) modified to handle cool star opacities using an opacity sampling technique for the bound-bound transitions (Johnson et al. 1980; Johnson et al. 1988; Brown et al. 1989). These models will then be used as input to an updated version of the Bowen hydrodynamic code (Bowen 1988), modified to improve the calculation of atomic and molecular opacities, and dust formation. Details of these modifications will be supplied in a future paper.

The hydrodynamic models representative of each star will then be used in the non-LTE (NLTE) code PANDORA (Vernazza, Avrett, & Loeser 1973 & 1976 & 1981; Luttermoser et al. 1989; Luttermoser 1992; Luttermoser & Johnson 1992; Luttermoser et al. 1994) to determine NLTE level densities and emergent synthetic spectra scaled to the angular size of the stars in our sample as determined from the PTI data. Finally the output generated by PANDORA will be used as input to the DUSTY code (Ivezic, Nenkova, & Elitzur 1997, Ivezic et al. 1997), using appropriate dust chemical types, in order to model the circumstellar environment around these stars.

Once the modeling is complete, the output of our calculations will be compared to the observed spectra and empirical data determined in the first stage of our analysis. Should a good fit be found, the depth of formation of various features can be determined as well as an understanding of atmospheric structure changes during a pulsation cycle. From this work, we should be able to get a fairly accurate measure of the mass loss for these stars. Should the comparison be lacking, then adjustments can be made to the input parameters, such as abundances, effective temperature, luminosity, mass, and radius and the models recalculated until a good fit is found. Finally, comparisons of the observed angular sizes with the determined stellar radius will enable us to accurately measure a distance to each star and constrain a period-luminosity relationship for Mira variables.

Acknowledgements: We thank the rest of our Spitzer Team (R. E. Stencel, R. R. Thompson, Z. Ivezić and J. Hora) for support of associated observing support related to this work and for their ongoing efforts toward the next steps. We also thank the PTI Collaboration and K. Rykoski for support of the interferometer time that made this study possible. This paper has made use of the SIMBAD database, ADS Abstracts Service, AAVSO and AFOEV databases, and we thank the developers and maintainers of those very important community services. This work was financially supported through a NASA Spitzer grant for Program GO 50717.

References:

Alvarez, R. et al., 1997, A&A, 327, 656.
Bowen, G.H. 1988, ApJ, 329, 299.
Brown, J.A., Johnson, H.R., Alexander, D.R., Cutright, L., & Sharp, C.M. 1989, ApJS, 71, 623.
Busso, M., Gallino, R. & Wasserburg, G. J., 1999, ARA&A, 37, 239.
Campbell, L., 1926, Annals of the Harvard Coll. Obs., 79, 87-158.
Castelaz, M.W., Luttermoser, D.G., Caton, D.B., & Piontek, R.A., 2000, AJ, 120, 2627.
Castelaz, M.W. & Luttermoser, D.G. 1997, AJ, 114, 1584.
Catchpole, R. M & Feast, M. W., 1971, MNRAS, 154, 197.
Colavita, M. M. et al, 1999, ApJ, 510, 505.
Comoretto, G. et al., 1990, A&AS, 84, 179.
Creech-Eakman, M. J. & Thompson, R. R., 2009, in The Biggest, Baddest, Coolest Stars, ed. by D. Luttermoser, B. Smith & R. Stencel, ASP Conf. Series, 412, 149.
Creech-Eakman, M. J., et al., 2009, in Stellar Pulsation: Challenges for Theory and Observations, AIP Conf. Series, 1170, 137.
Engels, D. & Heske, A., 1989, A&AS, 81, 323.
Espin, T. E. & Anderson, T. D., 1894, A&A, 13, 63.
Fleischer, A. J., Gauger, A. & Sedlmayr, E., 1992, A&A, 266, 321.
Habing, H. J., 1996, ARA&A, 7, 97.
Herwig, F., 2005, ARA&A, 43, 435.
Höfner, S., Feuchtinger, M. U., & Dorfi, E. A., 1995, A&A, 297, 815
Höfner, S., Gautschy-Loidl, R., Aringer, B., & Jørgensen, U. G. 2003, A&A, 399, 589
Hony, S. et al., 2009, A&A, 501, 609.
Houck, J. R., et al., 2004, SPIE, 5487, 62.
Iben, I., Jr, & Renzini, A., 1983, ARA&A, 21, 271.
Ivezić, Z., Nenkova, M., & Elitzur, M. 1997, "User Manual for DUSTY", http://www.pa.uky.edu/~moshe/dusty/
Ivezić, Z., Groenewegen, M. A. T., Men'shchikov, A., Szczerba, R. 1997, MNRAS, 291, 121.
Johnson, H.R., Bernat, A.P., & Krupp, B.M. 1980, ApJS , 42, 501.
Johnson, H.R., Luttermoser, D.G., & Faulkner, D.R. 1988, ApJ, 332, 421.
Jorissen, A. et al., 1993, A&A, 271, 463.

Kanbur, S. M., Hendry, M. A., & Clarke, D., 1997, MNRAS, 289, 428.
Kotnik-Karuza, D., et al., 2006, A&A, 452, 503.
Knapp, G. R., et al., 2003, A&A, 403, 993.
Kurayama, T. Sasao, T. & Kobayashi, H., 2005, ApJ, 627, 49.
Kurucz, R.L. 1970, "ATLAS: A Computer Program for Calculating Model Stellar Atmospheres," SAO Special Report 309.
Kurucz, R.L. 1979, ApJS, 40, 1.
Lewis, B. M., Eder, J. & Terzian, Y., 1990, ApJ, 362, 634.
Lewis, B. M., 1997, AJ, 114, 1602.
Little-Marenin, I. R. & Little, S. J., 1988, ApJ, 333, 305.
Little-Marenin, I. R. & Little, S. J., 1990, AJ, 99, 1173.
Luttermoser, D. G. et al. 1989, ApJ, 345, 543.
Luttermoser, D.G. & Bowen, G.H. 1990, in Sixth Cambridge Workshop on Cool Stars, Stellar Systems, and the Sun, ed. G. Wallerstein, ASP Conf. Series, 9, 491.
Luttermoser, D.G. & Bowen, G.H. 1992, in Seventh Cambridge Workshop on Cool Stars, Stellar Systems, and the Sun, ed. M.S. Giampapa & J.A. Bookbinder, ASP Conf. Series, 26, 558.
Luttermoser, D. G. & Johnson, H. R., 1992, ApJ, 388, 579.
Luttermoser, D. G., Johnson, H. R. & Eaton, J., 1994, ApJ, 422, 351.
Luttermoser, D.G. 1996, in Ninth Cambridge Workshop on Cool Stars, Stellar Systems, and the Sun, ed. R. Pallavicini & A.K. Dupree, ASP Conf. Series, 109, 535.
Luttermoser, D.G. 2000, ApJ, 536, 923.
Luttermoser, D.G. 2009, in Proceedings of The Biggest Baddest, Coolest Stars, ed. D.G. Luttermoser, B.J. Smith, & R.E. Stencel, ASP Conf. Series, 412, 163.
Merrill, P. W., Sanford, R. F. & Burwell, C. G., 1933, PASP, 45, 306.
Merrill, P.W. 1940, Spectra of Long-Period Variable Stars, Univ. of Chicago Press, Chapter IV.
Noguchi, K., Sun, J. & Wang, G., 1991, PASJ, 43, 311.
Nowotny, W., Höfner, S., & Aringer, B., 2010, A&A, 514, 35.
Olnon, F. M et al., 1986, A&AS, 65, 607.
Pickering, E. C. & Fleming, W. P., 1905, ApJ, 21, 292.
Sivagnanam, P., Le Squeren, A. M., & Foy, F., 1988, A&A, 206, 285.
Sloan, G. C. & Price, S. D., 1998, ApJS, 119, 141.
Sloan, G. C., Little-Marenin, I. R. & Price, S. D., 1998, AJ, 115, 809.
Sloan, G. C. et al., 2011, ApJ, 729, 121.
Speck, A. K., et al., 1998, PhD Thesis, Univ. College, London.
Speck, A. K. et al., 2000, A&AS, 146, 437.
Speck, A. K. et al., 2006, ApJ, 650, 892.
Srinivasan, S. et al., 2010, A&A, 524, 49.
Stephenson, C. B., 1976, "A General Catalogue of S Stars", Publ. Warner Swasey Observatory, 2, 21.
Van der Hucht, K.A. & Koornneef, J. 1994, An Infrared Spectral Line List of Astrophysical Interest (2.4 – 200 microns), ISO-SWS, SRON|/MPE/KUL.
van Hoof, P. 1999, University of Kentucky Atomic Line List, http://www.pa.uky.edu/~peter/atomic/
Vardya, M. S., de Jong, T. & Willems, F. J., 1986, ApJ, 304, 29.

Vernazza, J. E., Avrett, E. H., & Loeser, R., 1973, ApJ, 184, 605.
Vernazza, J. E., Avrett, E. H., & Loeser, R., 1976, ApJS, 30, 1.
Vernazza, J. E., Avrett, E. H. & Loeser, R., 1981, ApJS, 45, 635.
Vlemmings, W. H. T. & van Landvelde, H. J., 2007, IAU Symposium, Astrophysical masers and their Environments, 242, 342.
Wallerstein, G. & Knapp, G. R., 1998, ARA&A, 36, 369.
Werner, M. W. et al., 2004, ApJS, 154, 1.
Whitelock, P. A., Feast, M. W. and van Leeuwen, F., 2008, MNRAS, 386, 313.